LNF-96/005

Theoretical analysis of x-ray-absorption spectra at the Silicon K and $L_{2,3}$ edges of Crystalline and Amorphous SiO_2

J. Chaboy, M. Benfatto, I. Davoli

Physical Review B, 52, 14,10014-10020, (1995)

Theoretical analysis of x-ray-absorption spectra at the silicon K and $L_{2,3}$ edges of crystalline and amorphous SiO_2

Jesús Chaboy
Instituto de Ciencia de Materiales de Aragón, Consejo Superior de Investigaciones Cientificas, Universidad de Zaragoza, 50009 Zaragoza, Spain

Maurizio Benfatto
Laboratori Nazionali di Frascati, Istituto Nazionale di Fisica Nucleare, 00044 Frascati, Italy

Ivan Davoli
Dipartimento di Fisica, Universitá di Camerino, via Madonna delle Carceri, 62032 Camerino, Italy
(Received 26 May 1995)

In this work we present the analysis of the x-ray-absorption spectra at the silicon $L_{2,3}$ and K edges in amorphous SiO_2 and α quartz. This analysis consists in the comparison between experimental data and several calculations based on multiple scattering theory. An extensive discussion is presented concerning the role of the final state potential needed to reproduce the experimental data. In particular, the effects of the cluster-size, exchange-correlation potential and the role played by self-consistent-field potential are discussed. The remarkable agreement between the theoretical computations and the experimental data allows us to identify the origin of the different features in the x-ray-absorption near-edge structure spectra.

I. INTRODUCTION

X-ray-absorption spectroscopy (XAS) has large applications as a technique for investigation of the structural and electronic properties of materials. Impressive progress of XAS investigations are not only due to the significant development of the synchrotron radiation sources and the experimental techniques, but also to the increasing accuracy of theoretical models and computer simulations in accounting for the photoabsorption process.

Since the work of Lee and Pendry,[1] multiple scattering (MS) theory has been widely applied to interpret the modulations of x-ray-absorption spectra. The development in recent years of computer simulation codes using the MS scheme has opened the possibility to extract accurate structural information from the XAS signals in a large variety of systems, specially in the high energy region of the absorption spectra, extended x-ray-absorption fine structure (EXAFS).[2,3]

Whereas this development leads to a remarkable good agreement between the theoretical simulations and the experimental data in the EXAFS region, the extraction of quantitative information about crystallographic and/or electronic structure from the low energy part of the absorption spectrum (XANES) is difficult because of the complexity of translating in a practical computer code the developments of the theoretical description of the photoabsorption process made in recent years.

Indeed, all the current computer codes use the so-called muffin-tin approximation with an exchange-correlation potential ranging from an X_α to a complex Hedin-Lundqvist one. This scheme has reached a high level of accuracy in reproducing the experimental XANES data for metallic and semiconductor systems. However, it presents several difficulties to treating mixed valence, or more general, systems having electronic configurational mixing. Also, the few calculations performed on insulating materials seem to indicate that these optical potentials are inappropriate to describe the correlation between the core-hole and the outermost electrons. Indeed, the low energy part of the absorption spectra (at about 10 eV above the edge) is not well reproduced, specially for what concerns the intensity and broadening of the exciton lines (if they are present). It is therefore of the utmost importance to perform a detailed analysis of XAS spectra in insulators in order to have a deeper insight into the origin of the disagreement between theory and experiment, that can lead to the proposition of new theoretical improvements which are able to overcome these difficulties.

Silicon dioxide, SiO_2, is one of the most interesting insulator materials showing a great applicability in many fields of technology such as optoelectronics, high precision time scale basis, or metal-oxide semiconductor devices. Due to this technological interest, considerable efforts have been devoted to the study of the electronic structure as well as to the local atomic structure of both crystal and amorphous SiO_2.[4–7] However, SiO_2 is one of the most difficult materials to describe theoretically due to the complexity of the bonding scheme.[4] Moreover, SiO_2 occurs in a wide variety of forms with only small energy differences between the forms, the basic structural unit in all them being a SiO_4 tetrahedron. The various forms of SiO_2 are obtained by linking the tetrahedra

0163-1829/95/52(14)/10014(7)/$06.00

together in different ways, the two most common forms studied being the crystalline α quartz and the amorphous a-SiO_2 ones. In the last few years, although the electronic structure of α quartz has been widely studied both theoretically and experimentally,[4–9] only a few studies have been reported concerning the conduction band, i.e., the empty density of states (DOS).[8–10] In this sense, several x-ray-absorption near-edge structure (XANES) experiments have been recently carried out as an attempt to gain information about the empty density of states in both a-SiO_2 and α quartz.[11–14] However, the analysis of the experimental spectra has been restricted to a fingerprint comparison with previous DOS calculations and to using the empirical Natoli rule[15] to tentatively assign the XANES structures to the different interatomic distances present in the solids.

For the first time we present here the combined study of the x-ray-absorption spectra at both the silicon $L_{2,3}$ and K edges in amorphous SiO_2 and crystalline α quartz. This analysis is based on the comparison between the experimental data at the two edges and several XAS-MS calculations performed by using different choices for both the cluster size around the photoabsorbing atom and for the final state potential. In particular, special attention has been paid to establish the improvements obtained by using self-consistent-field (SCF) methods to describe the final state potential and the different treatments of the exchange-correlation part, i.e., X_α, Dirac-Hara (DH), and Hedin-Lundqvist (HL) potentials.

II. EXPERIMENTAL COMPARISON

The experimental XANES spectra for a-SiO_2 and α quartz are reported in Fig. 1. The two uppermost curves correspond to the absorption at the Si K edge recorded at the SA32 station of the SUPER-ACO storage ring at the LURE synchrotron radiation facility in Orsay, with an energy resolution of 0.7 eV,[16] showing no significant difference from those previously reported.[12–14] The data displayed for the absorption at the Si $L_{2,3}$ edge have been taken from the literature.[13,17,18] It has to be noted that in both cases the experimental data are not background substracted so that the intensity ratio of the different XANES resonances may differ from the normalized one.

The Si K edge in a-SiO_2 shows a strong and narrow white line (A) and a broad structure at about 18 eV above the white line, (E). In the case of α quartz the same features are present on the spectrum but three other additional weak structures appear located at energies 4.3 eV (B), 7.5 eV (C), and 10.5 eV (D) above peak A. On the other hand, the Si $L_{2,3}$ in a-SiO_2 is characterized by the presence of a weak double-peaked white-line, followed by a narrow structure, (D), and a very broad structure at about 20 eV above the absorption threshold (F). Feature F is present in most of the Si $L_{2,3}$ absorption spectra of silicon compounds, whereas the presence of peak D is observed to depend strongly on the nature of the ligand atoms.[19,20] In fact, it is absent in the XANES spectra of crystalline Si, extremely weak in the case of a-Si_3N_4, and huge in the case of solid SiF_4.[19]

It is important to note that both Si K and $L_{2,3}$ XANES spectra in a-SiO_2 and α quartz are very similar, confirming the fact that the main shape of the XAS spectra is dominated by the contributions coming from the nearest-neighbor shell. Contrary to other cases, in crystalline SiO_2 the contribution from farther shells produces small modifications to the absorption spectra of the amorphous material. In particular, the height and width of both the white line and the broad structure at high energy remain unmodified, and only a few weak features appear between these main structures.

Different approaches have been used in the past to identify the origin of these features. Most of them are based on the fingerprint comparison between experimental spectra and DOS calculations coming from a band structure approach.[12–14] The main limitation of this analysis is due to the impossibility to account for the core-hole effect, which is strong and relevant in this case. In fact, DOS calculations are far from reproducing the experimental data. Moreover, several authors try to interpret the XANES spectra on the grounds of the Natoli rule that establishes a relation between the energy position of a resonance and the distance between the absorber atom and its neighbors. In this way, Bart *et al.*[12] have identified the features (from A to E) in the Si K-edge spectrum of α quartz as due to single scattering contributions coming from the neighbor atoms located within 5 Å from the central Si. However, such an assignment can be strongly questioned because the application of this

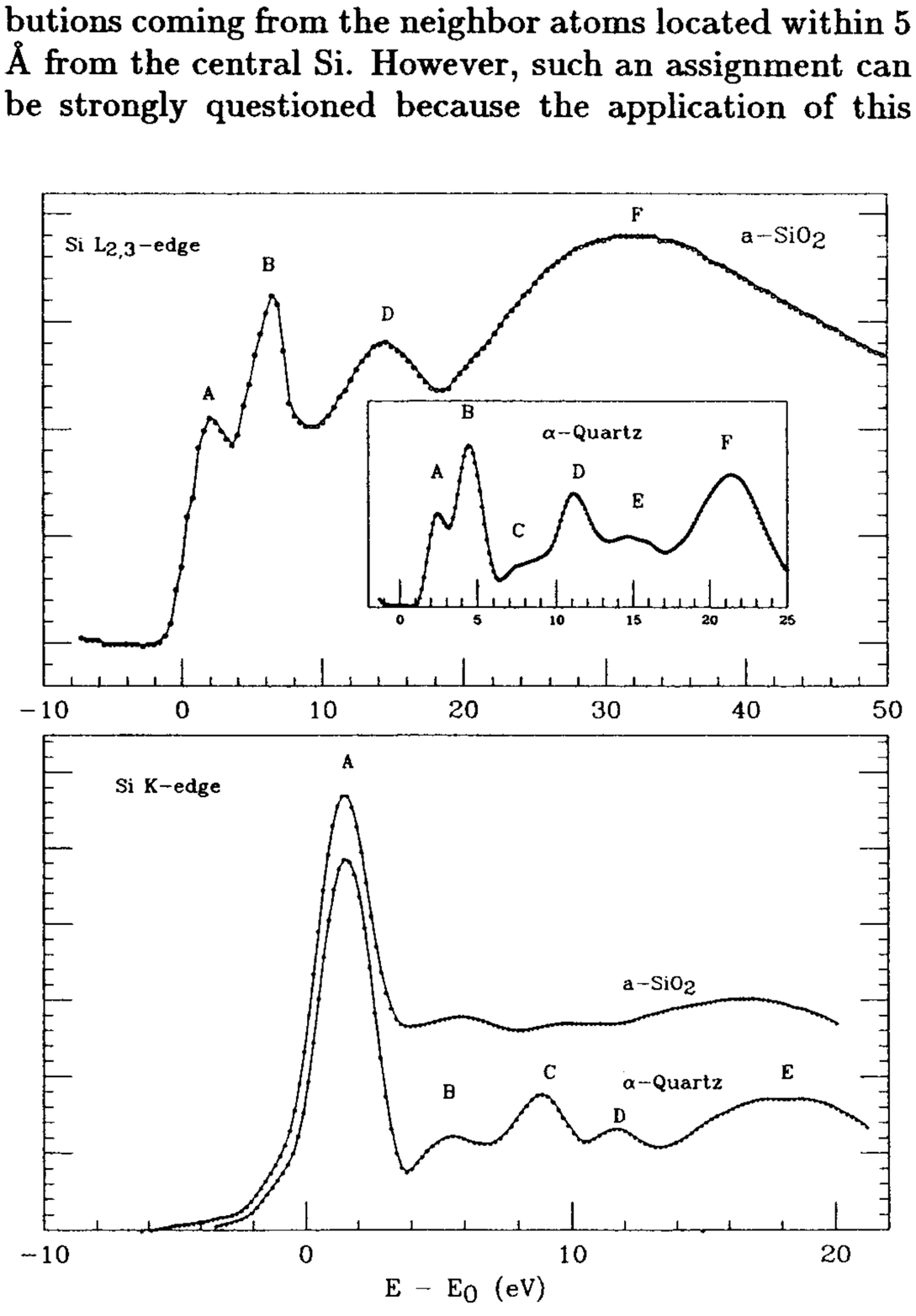

FIG. 1. In the bottom panel, the experimental XANES spectra at the Si K edge in a-SiO_2 and α quartz are reported (Ref. 16). The Si $L_{2,3}$-edge XANES spectrum for a-SiO_2, taken from Ref. 17, is shown in the top panel, whereas that of α quartz, taken from Ref. 13, is reported in the inset.

rule is based on the possibility to individuate the resonances stemming from the poles of the scattering path operator. They are essentially linked to the contributions coming from the first shell of atoms around the photoabsorber because the interference processes among the MS signals due to farther shells, i.e., shells having different distances, tend to destroy the presence and the influence of the poles. Under these constraints the application of the Natoli rule is essentially limited to the analysis of the first-neighbor shell, as many experimental data have confirmed.[15]

III. *AB INITIO* XANES CALCULATIONS

A. Theoretical method

In this section we will outline briefly the theoretical methods used for the calculations. The computation of the XANES spectra was carried out using the multiple-scattering code CONTINUUM (Ref. 3) based on the one-electron full-multiple-scattering theory.[1,21,22]

The atomic clusters of different size were approximated by a set of spherically averaged muffin-tin (MT) potentials built following the standard Mattheis prescription.[23] The muffin-tin radii were chosen according to the Norman criterion with 10% of overlapping factor.[24] Different choices were used to build the final state potential: (i) the same potential as for the ground state; (ii) screened $Z+1$ approximation, and (iii) self-consistent-field potential. Regarding the exchange and correlation part of the final state potential we have used three different types: X_α, the energy-dependent Hedin-Lundqvist complex potential, and the energy-dependent Dirac-Hara exchange potential. A complete discussion of the above methods exceeds the nature of this paper and can be found in Refs. 22, 25–28.

In order to obtain the self-consistent-field potential for both excited and ground states, due to the impossibility to build SCF potentials for clusters with a large number of atoms, we have stabilized a small cluster around the photoabsorber, i.e., silicon and first oxygen neighbors in tetrahedral coordination. This cluster has been embedded into the larger ones in order to perform the MS calculations, a procedure that has been previously shown to be successful on extended systems.[29,30]

B. Si *K* edge

Figure 2 reports the calculation of the Si K-edge XANES spectra obtained by using different cluster sizes around the photoabsorber with the α quartz geometrical coordination. The final state potential has been built on the basis of $Z+1$ and X_α approximations. The simulation performed for a small cluster of 19 atoms covering up to 4 Å around central Si shows a strong peak at the threshold and a broad structure located at about 18 eV above the white line. This result is also obtained by using even smaller clusters and is in agreement with the experimental data for a-SiO_2. Increasing the cluster size, the XANES profile exhibits the raising of new features between the white line and peak E. At the same time, peak E splits into two components (E_1, E_2), in agreement with the experimental spectra of α quartz, thus indicating the long-range origin of these features (B, C, D) that are not present in a-SiO_2. This result points out the invalidity of previous analyses, based on the use of Natoli's rule, which assign the origin of these features to scattering processes within the first 5 Å sphere around the central Si. Indeed, our calculations show the need to take into account up to 7 Å to reproduce feature D in the experimental spectra. Despite the good agreement obtained in reproducing all the features present in the experimental spectra, our calculation fails to reproduce both the width of the white line and the intensity ratio of structures B, C, and D.

In order to analyze this discrepancy we have performed other calculations using various final state potentials; the results are displayed in Fig. 3 for different cluster sizes. The lowermost curves show the comparison between the theoretical simulations performed on a 4 Å cluster by using X_α, $Z+1$, and SCF final state potentials, obtained as described above. The XANES profile is essentially the same, as regards the number and energy position of the features, but there is a strong difference from the width and height of the white line. In fact, the SCF calculation gives rise to a narrower and higher white line resembling the experimental data. This result points out both the local nature of this type of resonance and its relationship with the formation of an exciton state due to the presence

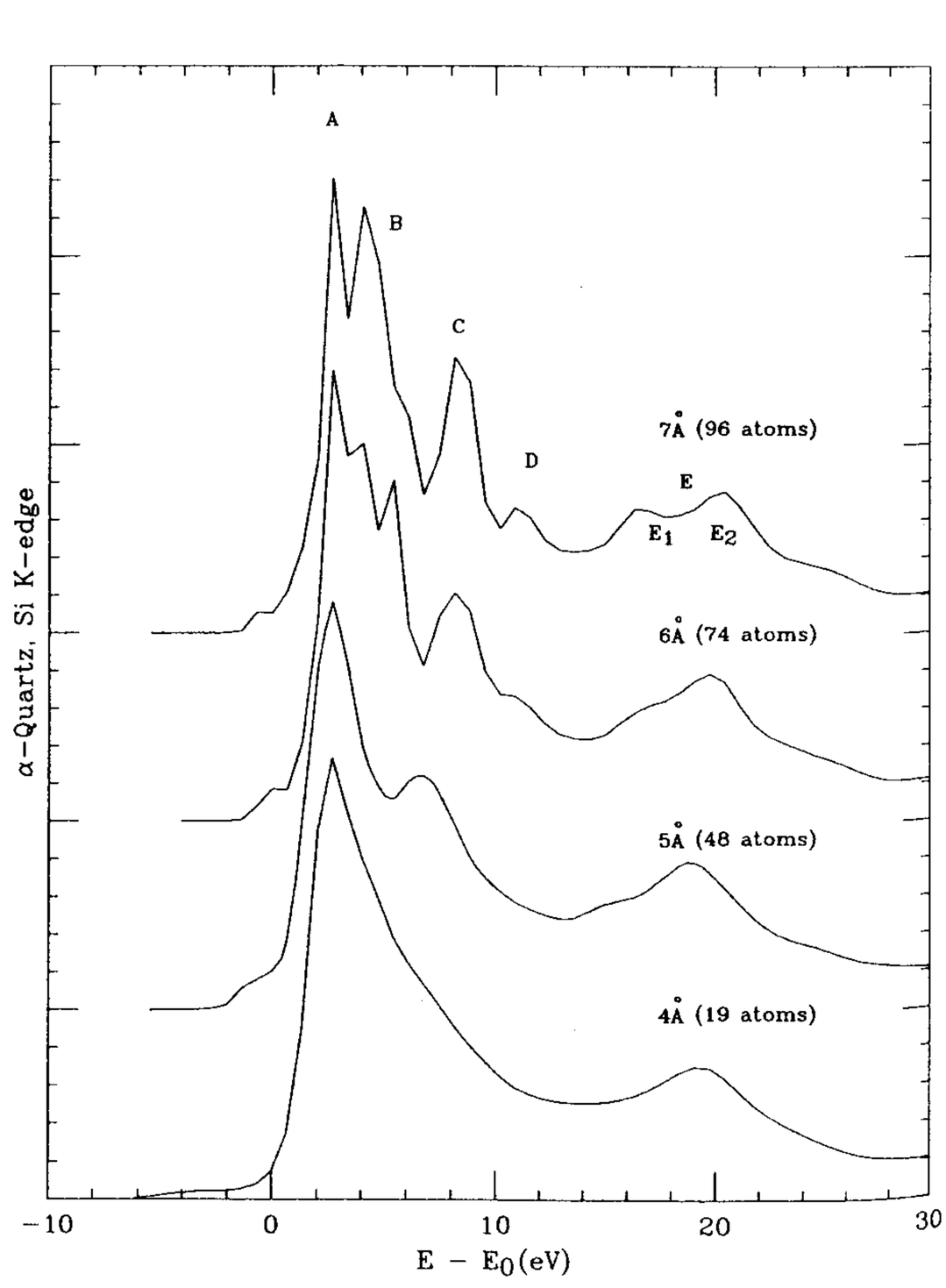

FIG. 2. Comparison between the theoretical Si K-edge XANES spectra performed for crystalline SiO_2 by using X_α potential and different cluster sizes.

of the core hole.[31]

The same comparison performed for a 7 Å cluster is reported in the uppermost curves of Fig. 3. For comparison we have also included the calculation obtained by using for the final state potential the same as for the ground state, i.e., without any core hole. As is clearly shown in the figure, the absence of the core hole produces a very drastic change of the first 10 eV of the absorption spectrum. In particular, the white line is completely destroyed and the intensity ratio of features B, C, and D is far from the experimental one. The best agreement with the experimental spectra is achieved by a SCF treatment of the final state potential. The height and the width of the white line resembles the experimental data and also the higher energy features are reproduced. Notwithstanding this noticeable agreement the intensity of feature B, which is strongly affected by its proximity to the white line, is not properly reproduced. On the contrary, the other features are well reproduced both in the energy position and intensity ratio. It should be noted that the use of different final state potentials induces modifications essentially in the first 15 eV, in agreement with the excitonic nature of this part of the spectra.

One of the possibilities to improve the theoretical simulation may be the use of different exchange-correlation contributions to the final state potential, due to the fact that they produce modifications on the energy separation between the various resonances. To this end, we report in Fig. 4 the comparison between calculations obtained by using different choices of the exchange-correlation potentials (ECP). The three computations are very similar for what concerns both the number of features and their intensity ratio. However, the use of the Dirac-Hara ECP leads to an increase of the white-line width and therefore to the poorest agreement with the experimental result. No significant improvement in the calculations has been obtained by using Hedin-Lundqvist ECP. Moreover, we have found that the complex part of the HL potential produces an excessive electron damping in such a way that features between the white line and peak E completely disappear (for the sake of brevity we do not show any figure reporting the result of this calculation).

To summarize, we address the need to use large clusters to account for the Si K-edge XANES spectra of α quartz ($\approx$7 Å) and the use of SCF potentials to reproduce correctly the first part of the spectra, strongly affected by the presence of the core exciton, although some problems remain concerning the width of the white line. As a final remark, the best agreement with the experimental data has been obtained by using X_α or real HL exchange-correlation potentials, being noticeable the failure of the complex part of the Hedin-Lundqvist ECP in accounting for the electron damping in these systems.

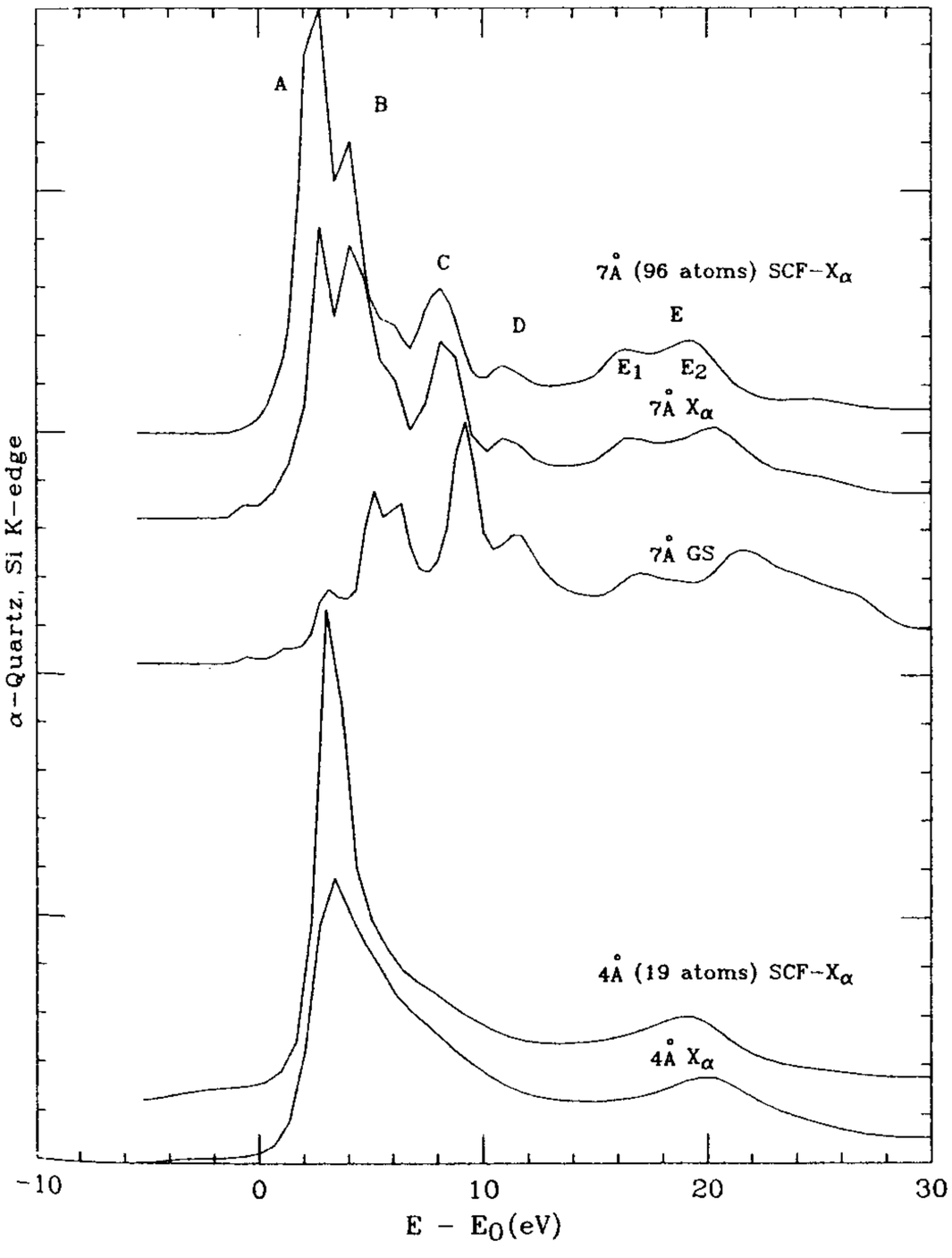

FIG. 3. Calculated Si K-edge spectra for α quartz performed on two different clusters and by using different potentials.

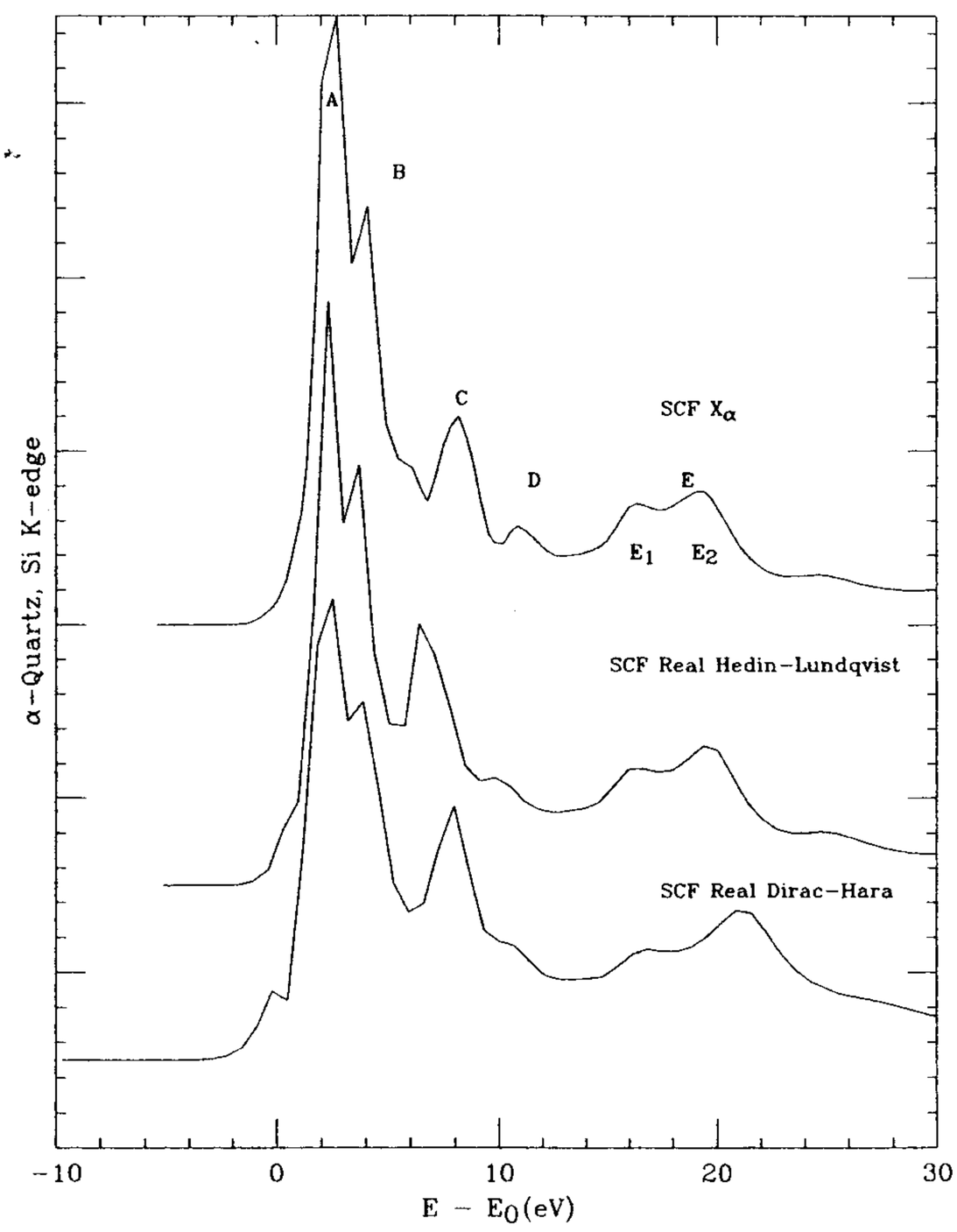

FIG. 4. Theoretical XANES simulation for the Si K edge in α quartz by using self-consistent-field X_α, real Hedin-Lundqvist, and real Dirac-Hara ECP potentials.

C. Si $L_{2,3}$ edges

Taking advantage of the above results, we have performed the analysis of the Si $L_{2,3}$ in both a-SiO_2 and crystalline α quartz. Figure 5 reports the calculation performed for the one-shell cluster using a SCF X_α final state potential. The calculation shows a remarkable good agreement with the experimental data of a-SiO_2, reproducing the double-peaked white line, the narrow structure D, and the broad structure at about 20 eV above the absorption threshold (see Fig. 1 for details). The symmetry decomposition of the calculated cross section allows us to single out the origin of the different structures in the absorption spectrum. The broad feature at about 20 eV above the edge (peak F) belongs to the d-like t_2 representation while peak D comes from the e representation component of the total cross section and it is due to a d-shape resonance resulting from the ligands. The white line is composed of two contributions, the most intense coming from transitions to d-like states (t_2 representation) and the other coming from transitions to s-like states (a_1 representation). This result indicates that the p-s channel is not negligible in this case and must be taken into account to reproduce correctly the double-peaked white line.

Contrary to the Si K-edge case, the use of SCF final state potential is not crucial to obtain a good reproduction of the experimental spectra. Indeed, the calculation performed by using the same potential for the final state as for the ground state reproduces well the XANES profile, the only appreciable difference being the intensity of both peak C and the d-like component of the white line. A $Z+1$ calculation also gives rise to the same results. This trend points out to a different nature of the absorption white line that, contrary to the Si K edge, cannot be associated to the formation of a core-exciton state, as is demonstrated by the rather good reproduction of the experimental spectra obtained by using the ground state potential.

Finally, Fig. 6 reports the theoretical simulation performed for the Si $L_{2,3}$ edges of α quartz. The two weak peaks below and above feature D only appear when using a cluster of 7 Å around central Si, indicating their long-range-order nature. Our calculations also report the existence of two additional peaks above the broad structure F, also due to long-range-order effects. As for the K edge, the best agreement with the experimental data is achieved by using the real HL exchange-correlation potential. Also in this case the complex part of the Hedin-Lundqvist ECP introduces an excessive electron damping.

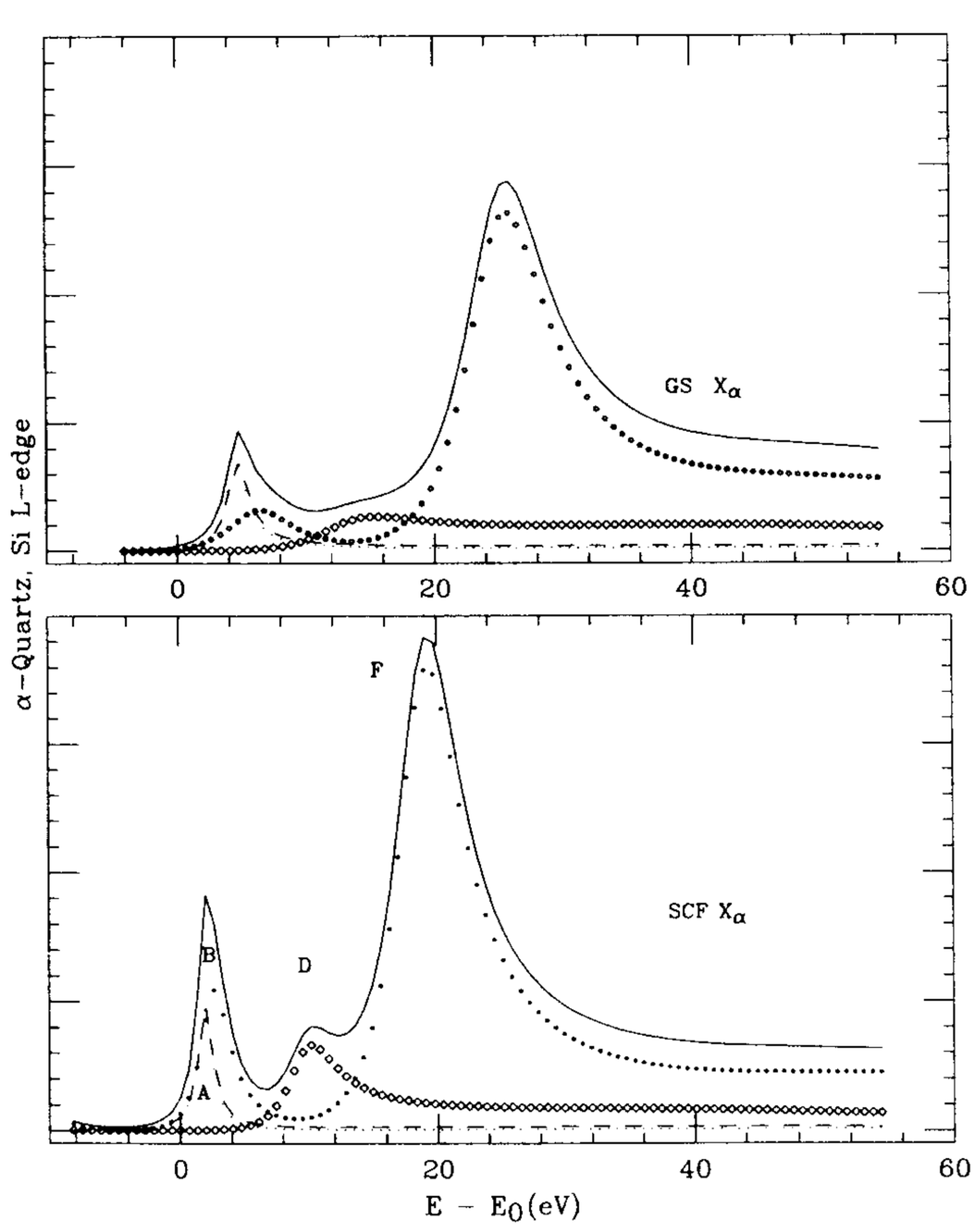

FIG. 5. Theoretical Si $L_{2,3}$ in a-SiO_2 calculation performed for the one-shell cluster using SCF X_α as the final state potential (bottom panel) and the same one as for the ground state (top panel). The symmetry decomposition of the calculated cross section is also shown: d-like t_2 (o) and e representations (◇); s-like a_1 representations (dashed line).

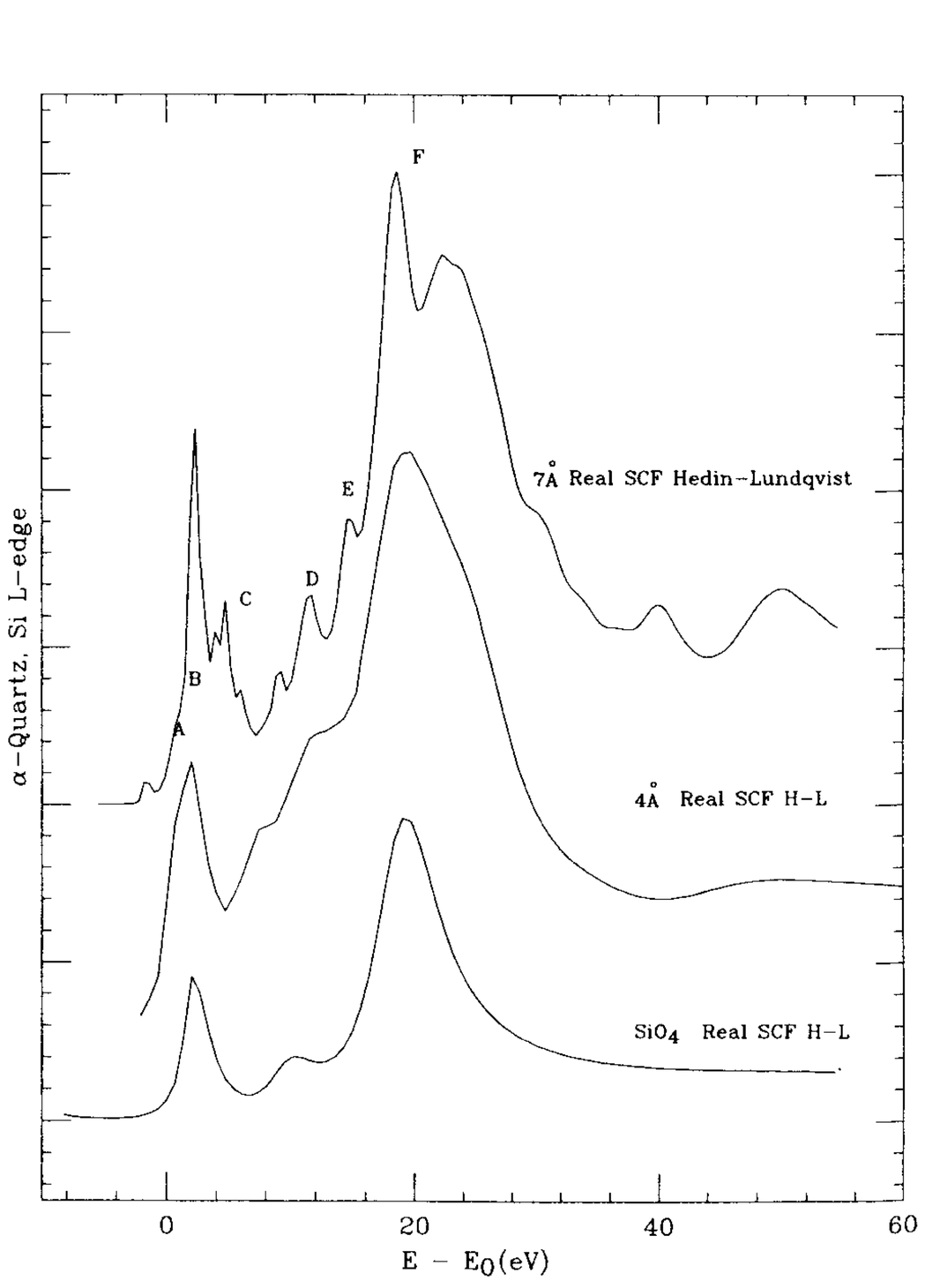

FIG. 6. Comparison between the theoretical Si $L_{2,3}$ performed for α quartz by using real SCF-HL ECP potentials and different cluster sizes.

IV. SUMMARY AND CONCLUSIONS

We have presented in this work a combined study of the x-ray-absorption spectra at both the silicon $L_{2,3}$ and K edges in amorphous SiO_2 and crystalline α quartz.

The comparison between the experimental data at the two edges and different XAS-MS calculations has demonstrated the need to use large clusters, $\approx$7Å around central Si, to reproduce the experimental spectra of α quartz, whereas XANES spectra of a-SiO_2 is well reproduced by using small clusters of SiO_4. Moreover, the theoretical calculations performed for clusters of different size, i.e., adding step by step the contribution of the different coordination shells, leads to the unambiguous identification of the origin of all the features present in the XAS spectra.

In the case of the Si K edge, the use of the SCF-HL potential in the *ab initio* calculations is found to be crucial to account for the strong white line exhibited by the experimental spectra for both amorphous and crystalline SiO_2. This particular structure is associated to the existence of an exciton state induced by the 1s core hole. On the contrary, this effect is not present at the Si $L_{2,3}$ edges, in which the use of SCF final state potentials is not as essential to obtain a good reproduction of the experimental spectra.

Regarding the K edge, our calculations reproduce all the features in the experimental spectra, although some problems remain when their intensity and width are below 10 eV, i.e., in the white-line region. The agreement between the experiment and the computations is remarkably good for that concerns the energy separation between the different XANES resonances. The fact that the white-line region is not well reproduced, both in width and intensity, is clearly associated to its excitonic nature, which cannot be correctly described by the current one-particle formalism used for the XANES calculations. On the other hand, the theoretical calculation of the $L_{2,3}$ edges is more relaxed. The sensitivity on the selection of the different final state potentials is far from critical and a good reproduction of the experimental data, including also the white-line region, has been obtained. It should be noted, however, the need to include explicitly in the calculation the contribution of the p-s channel, which is usually neglected in the literature.

During the multiple-scattering *ab initio* calculations we have tested different exchange and correlation possibilities to construct the final state potentials. The best agreement with the experimental data has been obtained by using X_α or real HL exchange-correlation potentials. Contrary to the case of metals and semiconductors, in which the HL potential, with its energy-dependent exchange and its imaginary part, is able to reproduce rather accurately the experimental spectra, the failure of the complex part of the Hedin-Lundqvist ECP to account for the electron damping in our systems, a result that current investigations show to be a general trend for insulating materials should be noted.

ACKNOWLEDGMENTS

This work was partially supported by Diputación General de Aragón DGA PCB09-93, Spanish CICYT MAT93-0240C04 and SAB94-0173 grants, and by the INFN-CICYT agreement. One of us (M.B.) would like to thank the U.E.I. V of the Instituto de Ciencia de Materiales de Aragón for the warm and friendly hospitality extended during the period in which this work was carried out. We wish also to acknowledge A. M. Flank for providing us with the experimental Si K-edge spectra.

[1] P.A. Lee and J.B. Pendry, Phys. Rev. B **11**, 2795 (1975).
[2] P. Durham, J.B. Pendry, and C.H. Hodges, Comput. Phys. Commun. **40**, 421 (1986); J. Mustre de Leon, J.J. Rehr, S.I. Zabinsky, and R.C. Albers, Phys. Rev. B **44**, 4146 (1991); J.J. Rehr, J. Mustre de Leon, S.I. Zabinsky, and R.C. Albers, J. Am. Chem. Soc. **113**, 5315 (1991).
[3] C.R. Natoli and M. Benfatto (unpublished); M. Benfatto, C.R. Natoli, A. Bianconi, J. Garcia, A. Marcelli, M. Fanfoni, and I. Davoli, Phys. Rev. B **34**, 5774 (1986).
[4] J.R. Chelikowsky and M. Schlutter, Phys. Rev. B **15**, 4020 (1977).
[5] N. Binggeli, N. Troullier, J.L. Martins, and J. Chelikowsky, Phys. Rev. B **44**, 4771 (1991).
[6] S.T. Pantelides and W.A. Harrison, Phys. Rev. B **13**, 2667 (1976).
[7] R.B. Laughling, J.D. Joannopoulos, and D.J Chadi, Phys. Rev. B **20**, 5228 (1979).
[8] W.Y. Ching, Phys. Rev. B **26**, 6610 (1982); **26**, 6622 (1982); **26**, 6633 (1982).
[9] R.P. Gupta, Phys. Rev. B **32**, 8278 (1985).
[10] M. Azizan, R. Baptist, A. Brenac, G. Chauvet, and T.A. Nguyen Tan, J. Phys. (Paris) **48**, 81 (1987).
[11] I. Davoli, E. Paris, S. Stizza, M. Benfatto, M. Fanfoni, A. Gargano, A. Bianconi, and F. Seifert, Phys. Chem. Mineral. **19**, 171 (1992).
[12] F. Bart, F. Jollet, J.P. Duraud, and L. Douillard, Phys. Status Solidi B **176**, 163 (1993).
[13] D. Li, G.M. Bancroft, M. Kasrai, M.E. Fleet, X.H. Feng, K.H. Tan, and B.X. Yang, Solid State Commun. **87**, 613 (1993).
[14] F. Jollet and C. Noguera, Phys. Status Solidi B **179**, 473 (1993).
[15] C.R. Natoli, in *EXAFS and Near Edge Structure*, Proceedings of the International Conference, edited by A. Bianconi, L. Incoccia, and S. Stipcich, Springer Series in Chemical Physics Vol. 27 (Springer, Berlin, 1983), p. 43.
[16] P. Lagarde and A.M. Flank, J. Phys. (Paris) **47**, 1389 (1986).
[17] F.C. Brown, R.Z. Bachrach, and M. Skibowski, Phys. Rev. B **15**, 4781 (1977).
[18] Y. Iguchi, Sci. Light (Tokyo) **26**, 161 (1977).
[19] I. Waki and Y. Hirai, J. Phys. Condens. Matter **1**, 6755 (1989).
[20] D.G.J. Sutherland, M. Kasrai, G.M. Bancroft, Z.F. Liu, and K.H. Tan, Phys. Rev. B **48**, 14 989 (1993).
[21] P.A. Lee and J.B Pendry, Phys. Rev. B **15**, 2862 (1977).
[22] C.R. Natoli and M. Benfatto, J. Phys. (Paris) Colloq. **47**, C8-11 (1986).

[23]L.F. Mattheis, Phys. Rev. A **133**, 1399 (1964); **134**, 970 (1964).
[24]J.G. Norman, Mol. Phys. **81**, 1191 (1974).
[25]M. Benfatto, in *2nd European Conference on Progress in X-ray Synchrotron Radiation Research*, edited by A. Balerna, E. Bernieri, and S. Mobilio (Societá Italiana di Fisica, Bologna, 1990), p. 3.
[26]C.R. Natoli, M. Benfatto, C. Brouder, M. Ruiz-Lopez, and D.L. Foulis, Phys. Rev. B **42**, 1944 (1990).
[27]C.R. Natoli, in *X-ray Absorption Fine Structure*, edited by S.S. Hasnain (Ellis Horwood, Chichester, U.K., 1991).
[28]T.A. Tyson, K.O. Hodgson, C.R. Natoli, and M. Benfatto Phys. Rev. B **46**, 5997 (1994).
[29]Z.Y. Wu, M. Benfatto, and C.R. Natoli, Phys. Rev. B **45** 531 (1992).
[30]M. Pedio, M. Benfatto, S. Aminpirooz, and J. Haase, Phys Rev. B **50**, 6596 (1994).
[31]N. Nagashima, A. Nakano, K. Ogata, M. Tamura, K. Sugawara, and K. Hayakawa, Phys. Rev. B **48**, 18 257 (1993).